Enhancing learning of the Grad-Shafranov equation through scientific literature: Part 3 of a physics education series

A. Ojeda-González*[1] ⓘ, M. Cristaldo-Oliveira[1,5], L. Nunes dos Santos[1,2] ⓘ,
A.N. Laurindo Sousa[3] ⓘ, S. Pilling[1], V. Klausner[1] ⓘ, V. De La Luz[4], A. Prestes[1]

[1]Universidade do Vale do Paraíba, Instituto de Física e Astronomia, São José dos Campos, SP, Brasil.
[2]Universidade Federal de Mato Grosso do Sul, Departamento de Matemática, Aquidauana, MS, Brasil.
[3]Universidade Estadual do Maranhão, Centro de Estudos Superiores de Balsas, Departamento de Matemática, Balsas, MA, Brasil.
[4]Universidad Nacional Autónoma de México, Escuela Nacional de Estudios Superiores, Morelia, Michoacán, Mexico.
[5]Secretaria de Estado de Educação de Mato Grosso do Sul, Superintendência de Politicas Educacionais, Campo Grande, MS, Brasil.

The Grad-Shafranov (GS) equation is a fundamental tool extensively used in plasma physics, particularly in the context of magnetic confinement, notably in tokamaks for fusion energy research. This equation plays a crucial role in reconstructing magnetic field topology in plasma regions like the magnetopause and magnetotail, leading to the development of the GS reconstruction technique. In this third installment of our series, we explore the merger of the Yoon-Lui-2 and Yoon-Lui-3 generating functions, allowing for a deeper understanding of the core equation in Plasma Physics. Furthermore, this article provides a comprehensive summary of solutions previously presented in Parts 1 and 2. We investigate the behavior of magnetic islands positioned above either the X-axis or the Z-axis for specific parameter values and their impact on plasma confinement. The article concludes that the derived model offers a simpler, more stable, and easily analyzable solution for magnetic morphology. However, it is worth noting that the model's inflexibility in singularity positions may limit its adaptability to different scenarios. This article marks the conclusion of our physics education series dedicated to studying new specific solutions of the GS equation.
Keywords: Grad-Shafranov equation, Magnetic flux-ropes, Plasma confinement, Singularity analysis.

1. Introduction

The Grad-Shafranov equation (GS equation) [1, 2] is a powerful tool in plasma physics, widely used for studying phenomena like magnetic reconnection, plasma turbulence, and flux tubes in planetary magnetospheres [3, 4]. This equation is expressed as:

$$\frac{\partial^2 A_y}{\partial x^2} + \frac{\partial^2 A_y}{\partial z^2} = -\mu_0 \frac{d}{dA_y}\left(p(A_y) + \frac{B_y^2(A_y)}{2\mu_0}\right), \quad (1)$$

where A_y denotes the y-component of the magnetic vector potential, the term $p(A_y)$ corresponds to the kinetic pressure of the plasma, and B_y represents the y-component of the magnetic field. It plays a crucial role in magnetic confinement, particularly in tokamaks for fusion energy [5, 6]. The equation enables the reconstruction of magnetic field topology in plasma regions such as the magnetopause and magnetotail, leading to the development of the Grad-Shafranov

reconstruction (GSR) technique [7]. GSR has been instrumental in analyzing plasma structures, identifying previously unknown phenomena, and refining the technique for improved accuracy, including its extension to toroidal geometries [8–15]. Additionally, the specific GS equation has contributed to the development of new analytical solutions that accurately model realistic magnetospheric configurations [16–19], advancing our understanding of plasma physics and complex dynamics in the geospace [20–28].

In the preceding two parts of this series, we explored how to develop research work in Physics with the aid of specialized scientific literature in a particular area. For this purpose, we presented analytical solutions of the specific GS equation by combining different generating functions proposed by Yoon and Lui (2005). In Part-1 [29], we combined the Yoon-Lui-1 and Yoon-Lui-2 generating functions, providing students with a new approach to the analytical solution of this challenging equation. Next, in Part-2 [30], we further expanded our reasoning and explored the combination of the Yoon-Lui-1 and Yoon-Lui-3 generating functions,

---

* Correspondence email address: ojeda.gonzalez.a@gmail.com

offering readers another valuable perspective for solving the specific GS equation.

In this article, we continue our series (Part-3), exploring the combination of the Yoon-Lui-2 and Yoon-Lui-3 generating functions [31, Sections 8 and 9].

In the upcoming sections, we will delve into various aspects of our study on the specific GS equation and its analytical solutions. Firstly, in Section 2, we will provide an overview of the Yoon-Lui-2 and Yoon-Lui-3 solutions, exploring their key features and implications. Following that, in Section 3, we will outline the methodology employed in our investigation, detailing the techniques and procedures used to obtain our results. In Section 4, we will present the results of our study and engage in a thorough discussion, analyzing the implications and significance of our findings. Finally, in Section 5, we will draw conclusions based on our research and discuss potential avenues for future exploration in this area of research.

To enhance the understanding of this article, we have chosen to include two supplementary sections in the Appendix, as detailed below: in Section A, we provide a detailed summary of the solutions proposed in Parts 1 and 2, highlighting their significance within the scope of our study; and in Section B, we unfold the algebraic steps involved in the derivation of the new solution introduced in this manuscript.

2. Yoon-Lui-2 and Yoon-Lui-3 Solutions Overview

This section provides an overview of the Yoon-Lui-2 and Yoon-Lui-3 solutions, derived by Yoon and Lui (2005) using Walker's formula. The chosen generating function for the Yoon-Lui-2 solution is given by:

$$g(\zeta) = \zeta - \frac{a}{\zeta}, \qquad (2)$$

where a is a parameters and ζ is a complex variable.

Substituting this into "Walker formula" [32]:

$$\Psi(X, Z) = \ln\left[\frac{1 + |g(\zeta)|^2}{2|g'(\zeta)|}\right], \qquad (3)$$

and performing the calculations, we obtain the following solution for the normalized magnetic vector potential $\Psi(X, Z)$:

$$\Psi(X, Z) = \ln\frac{\left(R^2 + a\right)^2 + R^2 - 4aX^2}{2\left[\left(R^2 + a\right)^2 - 4aZ^2\right]^{1/2}}, \qquad (4)$$

where $R^2 = X^2 + Z^2$.

The singular points of the Yoon-Lui-2 solution can be calculated by analyzing the derivative of the generating function, given by:

$$|g'(\zeta)| = \left|\zeta - \frac{a}{\zeta}\right|' = \left|\frac{a}{\zeta^2} + 1\right|. \qquad (5)$$

Further manipulations lead to:

$$|g'(\zeta)| = \left(\frac{a}{\zeta^2} + 1\right)^{\frac{1}{2}}\left(\frac{a}{\zeta^{*2}} + 1\right)^{\frac{1}{2}}. \qquad (6)$$

By solving the equation $\nabla \ln |g'(\zeta)| = 0$ [33], we find the singularities given by:

$$\left(\frac{a^2 + 2a(X^2 - Z^2) + (X^2 + Z^2)^2}{(X^2 + Z^2)^2}\right)^{\frac{1}{2}} = 0. \qquad (7)$$

The singular points depend on the value of a. For $a > 0$, the singularities are $(0, +\sqrt{a})$ and $(0, -\sqrt{a})$. For $a < 0$, the singularities are $(-\sqrt{a}, 0)$ and $(+\sqrt{a}, 0)$. When $a = 0$, there are no singular points.

In summary, the Yoon-Lui-2 solution, represented by (4), exhibits a specific morphology in terms of magnetic islands and singularities. The solution presents a current structure with two stable magnetic islands above the X-axis. However, it also includes two undesirable magnetic singularities above the Z-axis. By increasing the parameter a, it is possible to eliminate the singularities, but the magnetic islands move away from the origin. In comparison to the Brittnacher and Whipple model [34], the Yoon-Lui-2 model provides an alternative approach. The key distinction of the Yoon-Lui-2 model lies in the finite cross-field currents at the magnetic islands [31].

The Yoon-Lui-3 solution is given by:

$$g(\zeta) = \frac{\zeta}{(1 - a^2\zeta^2)}, \qquad (8)$$

and

$$\Psi(X, Z) = \frac{1}{2}\ln\left(\frac{S(S + R^2)^2}{2T_0}\right), \qquad (9)$$

where $S = (1 - a^2R^2)^2 + (2aZ)^2$, $T_0 = (1 - a^4R^4)^2 + (4a^2XZ)^2$, and a is a parameter that can affect the morphology of the solution. The generating function $g(\zeta)$ is used to locate the singularities of the solution, which occur at $(0, \pm\frac{1}{a})$. The solution exhibits singular points above the Z-axis, which can approach the origin as the parameter a increases, resulting in a neutral X-point configuration. The phenomenon of coalescence occurs when the singular points come close together and merge into a single structure, making the solution interesting for studying plasma behavior. The solution and its morphology are illustrated in a density plot that shows the magnetic field projected onto the XZ Cartesian plane, as previously presented in our previous work [30] (Part 2).

3. Methodology

In this study, we aim to explore the synergy between the Yoon-Lui-2 and Yoon-Lui-3 generating functions through a new solution. Our approach involves a unique

mathematical transformation to combine these two generating functions and derive a new function.

To obtain the proposed solution, we begin by conducting a mathematical derivation to obtain the modified generating function. Subsequently, we substitute this generating function into the Walker formula, as presented in equation (3), and perform the necessary algebraic manipulations to derive the expression for $\Psi(X, Z)$.

4. Results and Discussion

To derive the new solution, it is necessary to perform a series of algebraic manipulations based on the generating functions known as Yoon-Lui-2 and Yoon-Lui-3. All the steps involved in this process are detailed in the Appendix, in Section B. The final expression of the new solution is presented in Equation (B.13), constituting the main scientific result of this manuscript.

The solution derived from equation (B.13) is applicable only for values of a that are less than or equal to 1. At $a = 1$, the denominator of the argument within the logarithm becomes zero, leading to a vertical asymptote in the function at this specific point. For values of a greater than 1, the argument of the logarithm turns negative, which renders the expression mathematically undefined. Within the valid domain of a, *i.e.*, $a < 1$, the function has only one singular point when R equals zero (a pole in the solution). This implies a single indeterminacy at the origin of the coordinate system. The singularity at $R = 0$ cannot be shifted by varying the parameter a. This characteristic is considered a limitation of the model when compared to the Yoon-Lui-2 and Yoon-Lui-3 models, where singularities can be shifted by varying the parameter a.

In the new solution presented in equation (B.13) (which we refer to as *model 3*), comparing it with the solutions discussed in Part 1 (*model 1*) [29] and Part 2 (*model 2*) [30], its simplicity becomes evident. This simplicity arises from the absence of dependence on the parameter ν. It is worth noting that *models 1* and *2* depended on ν because this parameter was present in the Yoon-Lui-1 solution. Furthermore, *models 1* and *2* also depended on the parameter a, making them more complex to analyze the magnetic morphology since they involved the dependence of both parameters ν and a. In the new solution we are presenting, the dependence is only on a, making it easier to analyze in terms of magnetic morphology.

To gain a more detailed understanding of the model's geometry, it is essential to present the results graphically, using the same type of visualization adopted in the two previous manuscripts [29, 30]. This approach enables the comparison of the new solution, if necessary, with the previous solutions. Figure 1 consists of four panels that differ only in the adopted value of the parameter a, as follows: panel a) $a = -0.05$; panel b) $a = -0.5$;

panel c) $a = -1.0$; and panel d) $a = -2.5$. Overlaying the vector field on the X–Z Cartesian plane with the magnitude of the Y-component of the current density (J_y) enables the identification of singular points, magnetic islands, X-points, and the current sheet, if present. All the structures mentioned in the previous sentence are observed in this model; the only consideration is to make an appropriate choice of the parameter a, as will be explained below.

We begin our analysis of this model by selecting a value for a between 0 and -1. In panel a), it is observed that for $a = -0.05$, two magnetic islands symmetrically emerge above the Z-axis. These islands compress the magnetic structure formed by the singular point located at the origin. The magnetic field lines in the contact region between each island and the singular point above the Z-axis are oriented in the same direction. At the top ($Z > 0$), the field in the contact region is oriented to the left of the plane, and in the bottom region ($Z < 0$), the orientation is to the right of the plane. However, symmetrically above the X-axis, two neutral X-points emerge. These neutral points cause the magnetic islands to merge as the parameter a approaches zero. In other words, when $a = 0$ (see Figures 1c and 2a), the magnetic islands disappear, and a cylindrical current sheet forms around the singular point.

The ideal configuration of the magnetic islands emerges when $a = -0.5$, as illustrated in panel b) of Figure 1. In the range from $a = -0.5$ to $a = -1$, the islands approach each other again, and at $a = -1$, as shown in panel c), they completely merge to create a cylindrical ring current around the origin. This ring current represents a current sheet and has a configuration similar to that found in the Yoon-Lui-1 solution, particularly when the parameter ν is set to, for example, $\nu = 4$. This reveals a peculiarity: although the model is derived from the Yoon-Lui-2 and Yoon-Lui-3 models, it does not exhibit the specific type of magnetic morphology characteristic of its predecessors.

Continuing our analysis, it is observed that when the value of a is less than -1, as exemplified by $a = -2.5$ (refer to panel d) in Figure 1), the magnetic islands always remain above the X-axis. In this scenario, the reduction of a results in a progressive compression of this structure, maintaining, however, the same geometric properties. It is worth noting that this solution exhibits some resemblance to the Yoon-Lui-2 model, where the islands alternate their location between the Z-axis and the X-axis, depending on the value of the parameter a. This behavior was not observed in the two solutions presented in the two articles preceding this one (*model 1* and *model 2*).

Figure 2 presents a graph similar to Figure 1, but with different values of the parameter a: in panel a) $a = 0$, in panel b) $a = 0.05$, and in panel c) $a = 0.5$. In panel a), the ring current configuration is the same as in Figure 1c. In panels b) and c), by varying a from 0 to a value close to 1, we obtain a configuration similar to
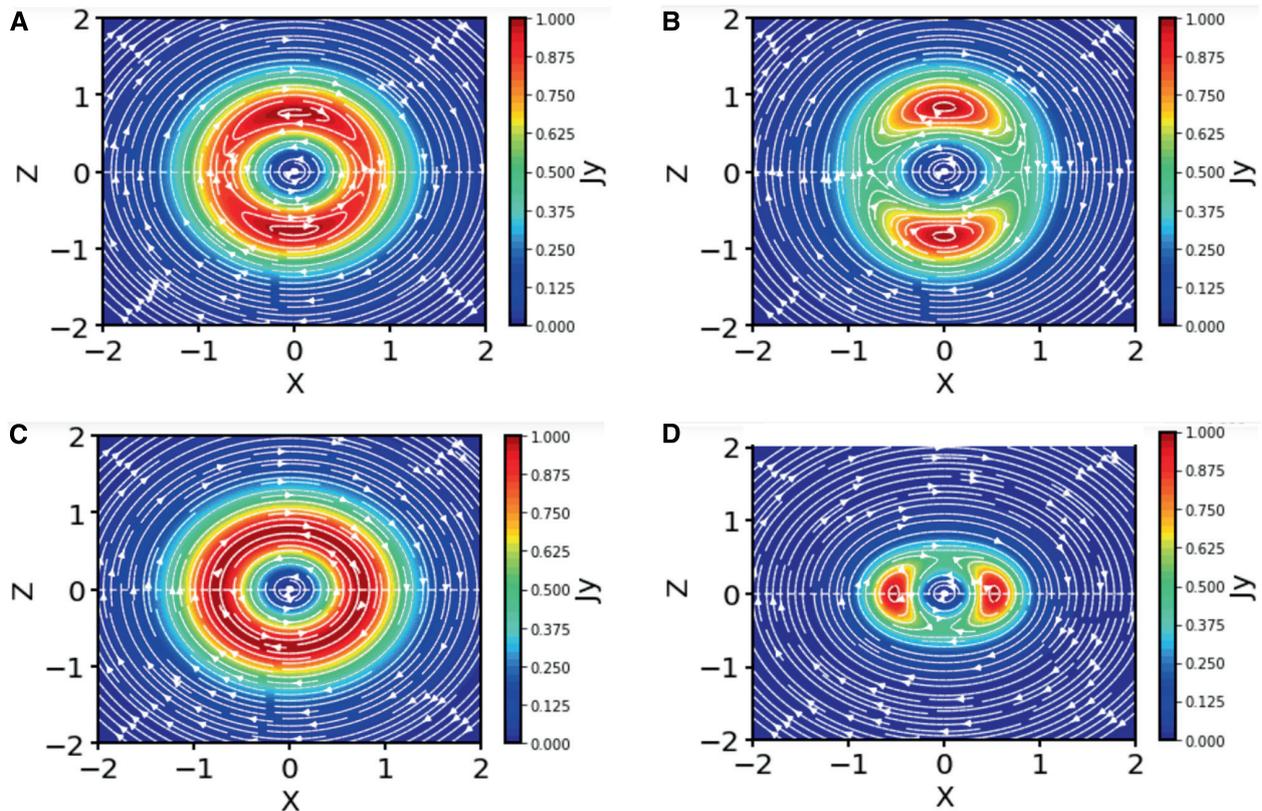
Figure 1: Graphs of the proposed solution (model B.13) for negative values of the parameter a as follows: $a = -0.05$ (panel a); $a = -0.5$ (panel b); $a = -1.0$ (panel c); $a = -2.5$ (panel d). Each panel shows the contour plot of the magnetic field with its respective orientation in the XZ plane, overlaid with the modulus of J_y. In all panels, there is a singular point at the origin of the coordinate system. In panels a) and b), two magnetic islands appear above the ordinate axis, and two neutral X points appear on the abscissa axis. When comparing panels a) and b) with panel d), a noticeable shift in axis placement is observed for both the islands and X points. Specifically, the X points transition from the X-axis to the Z-axis, while the islands undergo the reverse shift from the Z-axis to the X-axis. In panel c), there is a uniformly structured ring current around the origin, *i.e.*, a circular current sheet with cylindrical geometry along the Y axis.

that in Figure 1d: two magnetic islands above the X-axis, two neutral X-points on the Z-axis, and the singular point remains at the origin of the coordinate system. In panel b), with a value of a close to zero, the magnetic islands are observed in the process of merging or joining. In panel c), the islands are further apart, indicating a better magnetic structure.

When comparing the model (B.13) with the models (A.1) and (A.4) introduced by us in previous works, some distinct advantages and disadvantages stand out. One of the main advantages of the model (B.13) is its intrinsic simplicity. Unlike the models (A.1) and (A.4), which depend on two parameters, a and ν, the model (B.13) depends only on a, making it easier to analyze in terms of magnetic morphology. Additionally, the model (B.13) exhibits a fixed singularity at the origin, making it have well-defined magnetic structures (islands and X-points). However, this characteristic can also be observed in the models (A.1) and (A.4) by setting and $a = 1$ and $\nu = 1$ in both. It is important to note that, in these models, the position of some singularities can be adjusted by varying ν, thereby

offering greater flexibility in the modeling of magnetic structures. In the model (B.13), the position of the singularity remains unchanged, which limits the model's adaptability to different scenarios. Consequently, while the model (B.13) is characterized by its simpler and more stable formulation, it may not offer the same level of versatility as the models (A.1) and (A.4) in capturing a wide range of magnetic behaviors.

Regarding plasma confinement, the model (B.13) exhibits specific characteristics that are pertinent in certain contexts. The formation of magnetic islands above the X-axis or Z-axis for particular values of a can significantly impact plasma confinement and stability. These islands, while stable, may interact with the plasma in complex ways, affecting its dynamics and overall behavior. Additionally, anchoring the singularity at the origin establishes a central magnetic configuration, playing a pivotal role in the plasma's global stability by promoting the formation of X-points and subsequent current sheets. However, this model's inflexibility in altering singularity positions could restrict its adaptability to various plasma confinement scenarios. This contrasts with models (A.1)
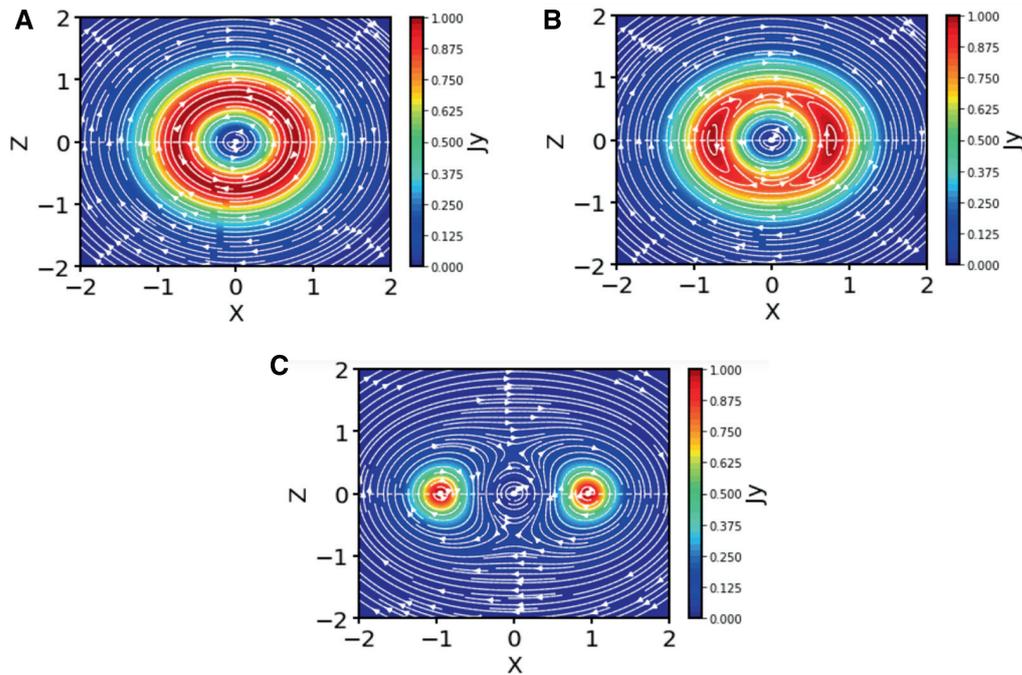
Figure 2: Graphs of the proposed solution (model B.13) for positive values of the parameter a: $a = 0$ (panel a); $a = 0.05$ (panel b); $a = 0.5$ (panel c). Each panel shows the contour plot of the magnetic field with its respective orientation in the XZ plane, overlaid with the modulus of J_y. In all panels, there is a singular point at the origin of the coordinate system. Two magnetic islands above the abscissa axis and two neutral X points on the ordinate axis appear in panels b) and c). In panel a), there is a uniformly structured ring current around the origin, *i.e.,* a circular current sheet with cylindrical geometry along the Y axis.

and (A.4), which allow for adjustments in singularity positions, thereby offering enhanced adaptability.

In the model (B.13), a particularly interesting case arises when $a = 0$ or $a = -1$, where the plasma is confined within a cylindrical current sheet forming around the origin. This behavior mirrors observations in the Yoon-Lui-1 model for $\nu = 1$, and in the model (A.4), a similar behavior is exhibited when $a = 1$ and $\nu = 4$. However, in the model (B.13), the cylindrical sheet is more distinctly defined upon examining the graph.

Regarding the phenomenon of coalescence [35], the model (B.13) was not specifically addressed in this context within the article. This omission is attributed to the lack of approximation or separation between the magnetic islands and singular points as the parameter a varies, which precludes the manifestation of this phenomenon.

5. Conclusion

This study introduces a simplified and stable solution for analyzing magnetic morphology in plasma physics, termed *model 3*, derived from the Yoon-Lui-2 and Yoon-Lui-3 generating functions using the Walker formula. Unlike the more complex *models 1* and *2*, *model 3* relies solely on the parameter a and features a stationary singularity at the origin, offering a novel approach to magnetic configuration analysis. This model reveals symmetric magnetic islands and a distinctive

cylindrical current sheet around the origin, impacting plasma confinement and stability in ways unique to this formulation.

Model 3 does not address the coalescence phenomenon due to its fixed singularity positions, highlighting a specific area where it diverges from previous models. Despite this, its straightforwardness and the novel insights it provides into magnetic configurations make it a valuable tool for both research and education in plasma physics.

This manuscript also underscores the educational value of *model 3* in theoretical learning within plasma physics, offering a resource for students and educators to explore advanced concepts through theoretical models, graphical visualization, and the study of magnetic phenomena. It contributes to the physics education series by presenting theoretical frameworks that enhance understanding of complex magnetic phenomena in plasma and space physics.

In concluding, *model 3* enriches the ongoing discourse in plasma physics with its unique approach to magnetic morphology, encouraging further exploration and research in the field.

Acknowledgments

Supplementary Material

The following online material is available for this article:

A. Reviewing the Solutions Presented in Part 1 and Part 2

In Part-1 of our series [29], we derived the solution for the Ψ function, in a specific plasma system. The equation for Ψ in this case is given by:

$$\Psi(X,Z) = \ln\left[\frac{R^{2(\nu+1)} + a^2 - 2aT^2 + R^4}{2\sqrt{R^{2\nu}\left[[(\nu-1)T^2 - a(\nu+1)]^2 + (\nu-1)^2 U^2\right]}}\right], \tag{A.1}$$

where the entered parameters are:

$$R^2 = X^2 + Z^2,\ U^2 = 4X^2Z^2,\ T^2 = X^2 - Z^2. \tag{A.2}$$

This simplified expression for Ψ is obtained after several algebraic manipulations of the original equation. To compute the singular points, we examine the derivative of the generating function $g(\zeta)$ and its representation in modulus form. From these equations, it is shown that the first condition for singular points is satisfied, that is, $\nabla \ln|g'(\zeta)| = 0$. Then we calculate the singular points by substituting $\zeta = X + iZ$ into the equation $|g'(\zeta)| = 0$. The solutions depend on the values of a and ν: If $a = 1$ and $\nu = 1$, the only singularity occurs at $\zeta = (0,0)$. For $\nu \neq 1$ and any value of a, the singularities are given by $\zeta = \zeta^* = \pm\sqrt{\frac{a(1+\nu)}{(\nu-1)}}$.

In this solution when increasing the parameter ν has a noticeable effect on the behavior of the system. As ν increases, the two singular points situated above the X axis gradually approach the magnetic islands. Consequently, the confinement of each magnetic island against the fixed singular point at the origin of the coordinate system becomes more effective.

The underlying reason for this phenomenon lies in the magnetic configuration itself. When a magnetic island is positioned between two singular points on each edge, these singular points interact with the magnetic field of the island. Importantly, the fields generated by the singular points and the island are directed in the same direction, thereby avoiding any magnetic reconnection [36–41]. As a result, the magnetic island experiences a tighter confinement between the singular points, which becomes increasingly pronounced as the parameter ν grows. Furthermore, this solution offers the flexibility to modify the positions of the external singular points while maintaining the fixed singular point at the origin and the magnetic islands unchanged.

Building on the findings presented in Part 1, Part 2 of our research series delved deeper into exploring the characteristics of Ψ and its connection to the plasma system. The obtained solution combines the generating functions of Yoon-Lui-1 and Yoon-Lui-3 through their division. The resulting generating function is expressed as:

$$g(\zeta) = \frac{\zeta^\nu}{\frac{\zeta}{1-a^2\zeta^2}} = \zeta^{\nu-1} - a^2\zeta^{\nu+1}, \tag{A.3}$$

where ν and a are constants. From this equation, we can derive the solution for Ψ, which is given by:

$$\Psi(X,Z) = \ln\left[\frac{1 + R^{2(\nu-1)}(a^4 R^4 - 2a^2 T^2 + 1)}{2\sqrt{R^{2(\nu-2)} \times}}\right.$$
$$\left. \times \frac{1}{\sqrt{[((\nu-1) - a^2(\nu+1)T^2)^2 + 4a^4(\nu+1)^2 U^2]}}\right]. \tag{A.4}$$

where R, T, and U are parameters previously presented in (A.2).

Continuing with the development, we calculate the singular points of the solution (A.4). The singularities occur at $(X,Z) = \left(\pm\sqrt{\frac{\nu-1}{a^2(\nu+1)}}, 0\right)$, for any ν different from -1 and a different from 0.

Some examples of singular points are:

- $\nu = 1.0$; $\zeta = (0,0)$;
- $\nu = 1.6$; $\zeta = (\pm0.48, 0)$;
- $\nu = 1.8$; $\zeta = (\pm0.53, 0)$;
- $\nu = 2.0$; $\zeta = (\pm0.58, 0)$;
- $\nu = 3.0$; $\zeta = (\pm0.71, 0)$;
- $\nu = 4.0$; $\zeta = (\pm0.77, 0)$.

These are just some examples of singular points, after fixing the parameters ν and a.

This solution revealed intriguing behavior. The magnetic field generated by the electrical current distribution exhibits distinct characteristics as the parameter values change. In the first configuration ($a = 1$, $\nu = 1$, and $\zeta = (0,0)$), a singular point is located at the origin, with two symmetric magnetic islands above the X-axis. This stable configuration proves advantageous for confining plasma within the islands.

As the parameter increases (i.e., $a = 1$, $\nu = 2$, and $\zeta = (\pm0.58, 0)$), the magnetic field morphology undergoes significant changes. Two equally spaced singular points

appear above the X-axis, accompanied by the singularity at the origin. The islands are displaced further away from the Z-axis, maintaining equal distances between each other.

In subsequent configurations (i.e., $a = 1$, $\nu = 4$, and $\zeta = (\pm 0.77, 0)$), the singular points continue to separate, resulting in increased confinement of the islands due to the influence of the external field. The surrounding islands assume a ring-like shape, while a central singularity with a structured magnetic field appears.

B. Algebraic Steps Involved in the Derivation of the New Solution

It is observed that increasing a in the Yoon-Lui-2 model separates the two islands, whereas in Yoon-Lui-3, the islands merge to form a single structure at the origin of the coordinate system. In this context, the curiosity arose to explore both effects by proposing a new generating function obtained from the multiplication of (2) and (8). Therefore, the generating function that will be used is:

$$g(\zeta) = \left(\zeta - \frac{a}{\zeta} \right) \left(\frac{\zeta}{1 - a^2 \zeta^2} \right)$$
$$= \frac{\zeta^2 - a}{1 - a^2 \zeta^2}. \quad (B.5)$$

According to the *Walker* formula presented in (3), it is necessary to obtain the square of the modulus of the derivative of (B.5). Therefore, we first obtain the derivative:

$$g'(\zeta) = \frac{2\zeta \left(1 - a^2 \zeta^2 \right) - (\zeta^2 - a)(-2a^2 \zeta)}{\left(1 - a^2 \zeta^2 \right)^2}$$
$$= \frac{2\zeta - 2a^2 \zeta^3 + 2a^2 \zeta^3 - 2a^3 \zeta}{\left(1 - a^2 \zeta^2 \right)^2}$$
$$= \frac{2\zeta \left(1 - a^3 \right)}{\left(1 - a^2 \zeta^2 \right)^2}, \quad (B.6)$$

then obtain the square of the modulus:

$$|g'(\zeta)|^2 = \frac{2^2 \left(1 - a^3 \right)^2 \zeta \zeta^*}{\left(1 - a^2 \zeta^2 \right)^2 \left(1 - a^2 \zeta^{*2} \right)^2}$$
$$= \frac{4 \left(1 - a^3 \right)^2 \left(X^2 + Z^2 \right)}{C}. \quad (B.7)$$

With C being:

$$C = \left[(1 - a^2 \zeta^2)(1 - a^2 \zeta^{*2}) \right]^2$$
$$= \left[1 - a\zeta^{*2} - a^2 \zeta^2 + a^4 \left(\zeta \zeta^* \right)^2 \right]^2$$

$$= \left[1 - a^2(\zeta^{*2} + \zeta^2) + a^4 (X^2 + Z^2)^2 \right]^2$$
$$= \left[1 - a^2(2X^2 - 2Z^2) + a^4 (X^2 + Z^2)^2 \right]^2$$
$$= \left[a^4 (X^2 + Z^2)^2 - 2a^2(X^2 - Z^2) + 1 \right]^2. \quad (B.8)$$

Therefore, equation (B.7) will be in the form:

$$|g'(\zeta)|^2 = \frac{4 \left(1 - a^3 \right)^2 \left(X^2 + Z^2 \right)}{\left[a^4(X^2 + Z^2)^2 - 2a^2(X^2 - Z^2) + 1 \right]^2}. \quad (B.9)$$

Where,

$$|g'(\zeta)| = \frac{2 \left(1 - a^3 \right) \sqrt{(X^2 + Z^2}}{a^4(X^2 + Z^2)^2 - 2a^2(X^2 - Z^2) + 1}. \quad (B.10)$$

Notice that according to (3), it is necessary to calculate $1 + |g(\zeta)|^2$ in the numerator of the logarithm argument. The mathematical development is as follows:

$$1 + |g(\zeta)|^2 = 1 + \left(\frac{\zeta^2 - a}{1 - a^2 \zeta^2} \right) \left(\frac{\zeta^{*2} - a}{1 - a^2 \zeta^{*2}} \right)$$
$$= 1 + \frac{(X^2 + Z^2)^2 - 2a(X^2 - Z^2) + a^2}{a^4(X^2 + Z^2)^2 - 2a^2(X^2 - Z^2) + 1}. \quad (B.11)$$

Continuing with the algebraic work and employing the variable changes presented in (A.2), we have:

$$1 + |g(\zeta)|^2 = \frac{(a^4 + 1)R^4 - 2a(a + 1)T^2 + (a^2 + 1)}{a^4 R^4 - 2a^2 T^2 + 1}. \quad (B.12)$$

Therefore, substituting (B.10) and (B.12) into (3), we have found the expression for the new solution:

$$\Psi(X, Z) = \ln \left[\frac{(a^4 + 1)R^4 - 2a(a + 1)T^2 + a^2 + 1}{4\sqrt{R^2}(1 - a^3)} \right]. \quad (B.13)$$

References

[1] H. Grad and H. Rubin, in: *Proceedings of the 2nd United Nations International Conference on the Peaceful Uses of Atomic Energy* (Geneva, 1958).

[2] V.D. Shafranov, Rev. Plasma Phys. **2**, 103, (1966).

[3] G. Ambrosino and R. Albanese, Control Systems IEEE **25**, 76 (2005).

[4] C.V. Atanasiu, S. Günter, K. Lackner and I.G. Miron, Phys. Plasmas. **11**, 3510 (2004).

[5] K. Lackner, *Computer Physics Communications* **12**, 33 (1976).

[6] P.J. Mc Carthy, Phys. Plasmas **6**, 3554 (1999).

[7] B.U.Ö. Sonnerup, H. Hasegawa, W.L. Teh and L.N. Hau, Journal Geophys. Res. **111**, A09204 (2006).

[8] H. Hasegawa, H. Zhang, Y. Lin, B. Sonnerup, S. Schwartz, B. Lavraud and Q. Zong, Journal Of Geophysical Research (Space Physics) **117**, eA09214 (2012).

[9] Q. Hu, Science China Earth Sciences **60**, 1466 (2017).

[10] L. Hau and B. Sonnerup, Journal Of Geophysical Research **104**, 6899 (1999).

[11] B. Sonnerup and W. Teh, Journal Of Geophysical Research (Space Physics) **114**, eA04206 (2009).

[12] H. Li, X. Feng, P. Zuo and Y. Xie, Science In China E: Technological Sciences **52**, 2555 (2009).

[13] A. Isavnin, E. Kilpua and H. Koskinen, Sol. Phys. **273**, 205 (2011).

[14] Q. Hu and B. Sonnerup, J. Geophys. Res. **107**, 1142 (2002).

[15] A. Ojeda-Gonzalez, V. Klausner, O. Mendes, M.O. Domingues and A. Prestes, Sol. Phys. **292**, 160 (2017).

[16] A. Ojeda-Gonzalez, M.O. Domingues, O. Mendes, M.K. Kaibara and A. Prestes, Braz. J. Phys. **45**, 493 (2015).

[17] M. Cristaldo-Oliveira, A. Ojeda-Gonzalez, L.N. Santos, A. Prestes and A.N. Laurindo-Sousa, Rev. Bras. Ensino Fis. **42**, e20200297 (2020).

[18] J.R. Kan, Journal Geophys. Res. **78**, 3773 (1973).

[19] J.R. Kan, Plan. Space Sci. **27**, 351 (1979).

[20] K. Arzner and M. Scholer, J. Geophys. Res. **106**, 3827 (2001).

[21] J. Birn and M. Hesse, J. Geophys. Res. **106**, 3737 (2001).

[22] U. Becker, T. Neukirch and K. Schindler, J. Geophys. Res. **106**, 3811 (2001).

[23] M. Hesse, J. Birn and M. Kuznetsova, J. Geophys. Res. **106**, 3721 (2001).

[24] M. Kuznetsova, M. Hesse and D. Winske, J. Geophys. Res. **106**, 3799 (2001).

[25] A. Otto, J. Geophys. Res. **106**, 3751 (2001).

[26] M. Shay, J. Drake, B. Rogers and R. Denton, J. Geophys. Res. **106**, 3759 (2001).

[27] Y. Ma and H. Zhang, in: *IEEE International Conference on Multimedia and Expo (ICME)* (Tokyo, 2001).

[28] P. Pritchett, J. Geophys. Res. **106**, 3783 (2001).

[29] A. Ojeda-Gonzalez, L. Santos, V. De La Luz, M. Cristaldo-Oliveira, A. Laurindo Sousa, A. Prestes, V. Klausner and S. Pilling, Rev. Bras. Ensino Fis. **45**, e20230104 (2023).

[30] L N. Santos, A. Ojeda-Gonzalez, V. De La Luz, V. Klausner, S. Pilling, A. Prestes, A.N. Laurindo Sousa and M. Cristaldo-Oliveira, Rev. Bras. Ensino Fis. **45**, e20230217 (2023).

[31] P.H. Yoon and A.T.Y. Lui, Journal Geophys. Res. **110**, A01202 (2005).

[32] G.W. Walker, Proc. R. Soc. Lond. A. **91**, 410 (1915).

[33] V. Génot, JGR Space Phys. **110**, A09214, (2005).

[34] M. Brittnacher and E. Whipple, JGR Space Phys. **107**, 1022 (2002).

[35] M. Bussac, R. Pellat, J. Soule and M. Tagger, Physics Letters A **105**, 51 (1984).

[36] R. Giovanelli, Nature **158**, 81 (1946).

[37] J. Dungey, Physical Review Letters **6**, 47 (1961).

[38] E. Zweibel and M. Yamada, Proceedings Of The Royal Society Of London Series A **472**, 20160479 (2016).

[39] T.D. Phan, J.P. Eastwood, M.A. Shay, J.F. Drake, B.U.Ö. Sonnerup, M. Fujimoto, P.A. Cassak, M. Øieroset, J.L. Burch, R.B. Torbert et al., Nature **557**, 202 (2018).

[40] D. Koga, W. Gonzalez, V. Souza, F. Cardoso, C. Wang and Z. Liu, JGR Space Phys **124**, 8778 (2019).

[41] V. Souza, D. Koga, W. Gonzalez and F. Cardoso, Braz. J. Phys **47**, 447 (2017).